

Self-excitation of microwave oscillations in plasma-assisted slow-wave oscillators by an electron beam with a movable focus

Yu. P. Bliokh,¹ G. S. Nusinovich,² A. G. Shkvarunets,² and Y. Carmel²

¹*Technion, Haifa, 32000, Israel*

²*Institute for Research in Electronics and Applied Physics, University of Maryland, College Park, Maryland 20742-3511, USA*

(Received 12 March 2004; published 7 October 2004)

Plasma-assisted slow-wave oscillators (pasotrons) operate without external magnetic fields, which makes these devices quite compact and lightweight. Beam focusing in pasotrons is provided by ions, which appear in the device due to the impact ionization of a neutral gas by beam electrons. Typically, the ionization time is on the order of the rise time of the beam current. This means that, during the rise of the current, beam focusing by ions becomes stronger. Correspondingly, a beam of electrons, which was initially diverging radially due to the self-electric field, starts to be focused by ions, and this focus moves towards the gun as the ion density increases. This feature makes the self-excitation of electromagnetic (em) oscillations in pasotrons quite different from practically all other microwave sources where em oscillations are excited by a stationary electron beam. The process of self-excitation of em oscillations has been studied both theoretically and experimentally. It is shown that in pasotrons, during the beam current rise the amount of current entering the interaction space and the beam coupling to the em field vary. As a result, the self-excitation can proceed faster than in conventional microwave sources with similar operating parameters such as the operating frequency, cavity quality-factor and the beam current and voltage.

DOI: 10.1103/PhysRevE.70.046501

PACS number(s): 41.85.Ja, 84.40.Fe, 52.75.-d

I. INTRODUCTION

For many sources of coherent microwave radiation, the self-excitation of oscillations and proper start-up scenarios are very important. Typically, the conditions for self-excitation of oscillations are quite different from the choice of parameters, which yield the maximum efficiency, or power, or gain, or bandwidth of the device. Therefore, to match these two stages, viz., self-excitation and optimal operation, a proper start-up scenario should be realized. (Problems of start-up scenarios in high-power gyrotrons operating in high-order modes were recently discussed in Ref. [1])

Self-excitation of oscillations in cavities of various microwave sources strongly depends on the relation between the cavity fill/decay time, Q/ω , (here Q is the cavity quality factor and ω is the oscillation frequency) and a typical rise time, t_{rise} , of the beam voltage and current in the beginning of operation. There are two limiting cases, viz., instant turn-on and slow turn-on, which we will discuss below. (Note that in regard to gyrotrons these cases were discussed in Ref. [2].)

Instant turn-on implies that the rise time of the electron beam current, t_{rise} , is much smaller than a typical decay time of the cavity:

$$t_{rise} \ll Q/\omega. \quad (1)$$

In this case, the beam current, I_b , reaches its nominal value, $I_{b,nom}$, practically instantly.

In general, the equation describing the electromagnetic (em) field excitation in the cavity can be derived from the wave equation and written as

$$\frac{dA}{dt} = \omega A [I\Phi' - 1/2Q], \quad (2)$$

where A is the amplitude of the em field, Φ' is the real part of the gain function, which will be considered below in the framework of the linear theory, i.e., without accounting for the saturation effects. Also in Eq. (2) I is the normalized beam current parameter proportional to the beam current. (For our present consideration, its exact definition does not matter, but later this parameter will be specified for pasotrons.) As follows from Eq. (2), the starting value of this parameter is equal to

$$I_{st} = 1/2\Phi'Q. \quad (3)$$

In the case of the instant turn-on the normalized beam current parameter (as well as the beam current itself) instantly reaches its nominal value, $I=I_{nom}$. Thus the solution of Eq. (2) can be written as

$$A(t) = A_0 \exp \left\{ \frac{\omega t}{2Q} \left(\frac{I_{nom}}{I_{st}} - 1 \right) \right\}. \quad (4)$$

So the growth rate of the em field amplitude in this case depends on the excess of the nominal current over its threshold value. This is a known case, which is simple but unrealistic. Typically, in microwave oscillators the opposite case takes place.

Slow turn-on is the case when the rise time of the beam current is much larger than the cavity decay time:

$$t_{rise} \gg Q/\omega. \quad (5)$$

For devices operating at frequencies from 1 GHz to 10 GHz and employing cavities with Q -factors on the order of 10^2 - 10^3 , the cavity decay time is in a nanosecond scale,

which is much smaller than typical rise times of the beam current in various pulsed microwave sources including the pasotrons where the current rise time is in the microsecond range. For instance, in pasotrons (the word ‘‘pasotron’’ is an acronym for plasma-assisted slow-wave oscillator) studied at Hughes Research Lab [3] and later at the University of Maryland [4], the operating frequency is about 1.3 GHz, the Q -factor is about several hundreds and the beam current rise time is about 10–20 microseconds. So, just the case of the slow turn-on is the case of the practical interest. In this case, the normalized beam current parameter in Eq. (2) should be treated as the function of time. Since the oscillations start to rise at the instant of time, t_{st} , when the beam current equals to its starting value, we can expand the time dependence of the beam current in the vicinity of t_{st} in a Taylor series:

$$I(t) = I(t_{st}) + \left. \frac{dI}{dt} \right|_{t_{st}} (t - t_{st}). \quad (6)$$

With this representation, Eq. (2) can be rewritten as

$$\frac{dA}{dt} = \frac{\omega}{2Q} A \left[\frac{1}{I_{st}} \left. \frac{dI}{dt} \right|_{t_{st}} (t - t_{st}) \right]. \quad (7)$$

The solution of Eq. (7) has the form

$$A(t) = A_0 \exp \left\{ \frac{\omega}{4Q} \frac{1}{I_{st}} \left. \frac{dI}{dt} \right|_{t_{st}} (t - t_{st})^2 \right\}, \quad t > t_{st}. \quad (8)$$

So, the growth rate of em oscillations is determined by the derivative $dI/dt|_{t_{st}}$. In most of the microwave sources, the temporal dependence of the beam current during the current rise can be approximated by the linear function

$$I_b(t) = \frac{t}{t_{rise}} I_{nom}. \quad (9)$$

Hence, in this case, the derivative $dI/dt|_{t_{st}}$ is simply I_{nom}/t_{rise} . Correspondingly, Eq. (8) can be rewritten as

$$A(t) = A_0 \exp \left\{ \frac{\omega}{4Q} \frac{I_{nom}}{I_{st}} \frac{(t - t_{st})^2}{t_{rise}} \right\}, \quad t > t_{st}. \quad (10)$$

In pasotrons, however, a typical time of the beam impact ionization, t_{ion} , is on the order of the beam current rise time, $t_{ion} \sim t_{rise}$ [3]. Therefore the ion focusing of the beam varies in time during the current rise. Correspondingly, during this time interval, the amount of the beam current entering the interaction space, $I_{b,int}$, is smaller than the total beam current extracted from the gun and therefore the temporal dependence of this portion of the beam current can be quite different from the linear dependence given by Eq. (9). As follows from Eq. (8), when

$$\left. \frac{dI_{b,int}}{dt} \right|_{t_{st}} > \left. \frac{dI_b}{dt} \right|_{t_{st}}, \quad (10a)$$

em oscillations grow faster than in the case of $I_{b,int} = I_b$ and vice versa. So, one should expect that the growth rate of em oscillations in pasotrons should depend on the processes of beam impact ionization of an initially neutral gas and on the beam focusing by created ions. Note that the temporal varia-

tion in the beam focusing not only changes the amount of beam current entering the interaction region, $I_{b,int}$, but also affects the starting current, which depends on the beam geometry, as will be discussed later.

In principle, the pasotrons are quite unique sources of microwave radiation because the beam focusing and transport is provided there by ions (in the absence of guiding external magnetic fields) in the regime known as the Bennett pinch [5]. However, some peculiarities of the beam pinching in pasotrons, which is a nonstationary process during at least the initial stage of ionization, can be explained [6,7] with the use of the known theory of optics of stationary paraxial electron beams [8,9]. This theory predicts that an electron beam with the negative generalized perveance,

$$K = \frac{eI_b}{mc^3 \beta^3 \gamma^3} (1 - \gamma^2 f), \quad (11)$$

has the focal plane located at the distance

$$z_f = 0.8a_0 \sqrt{|K|/2} \quad (12)$$

from the entrance. Here, in (11) β is the initial electron axial velocity normalized to the speed of light, γ is the electron energy normalized to the rest energy, and f is the charge neutralization factor, which is the ratio of the ion density to the electron beam density. Also, in Eq. (12) a_0 is the initial radius of the beam envelope; Eq. (12) is derived for the case when at the entrance all electrons propagate along the axis of the device. As follows from the processes discussed above, in pasotrons the generalized perveance given by Eq. (11) is variable, in contrast to the known stationary theory of beam optics [8,9], because in Eq. (11) not only the beam current I_b but also the charge neutralization factor vary during the beam current rise. This means that during this time interval, first, the beam will start to be focused when the ion density becomes high enough (corresponding condition of beam focusing, $f > 1/\gamma^2$, is known as Budker criterion [10]), and then the focal plane of the beam will move along the z -axis until the beam current and ion density reach their stationary values (see also [11]). Clearly, this motion of the focus and corresponding changes in the beam focusing can be important for pasotron self-excitation. This is because the temporal variations in the beam radial profile change the beam coupling to the slow space harmonic of the em wave, whose phase velocity is synchronous with electrons and whose field is localized near the slow-wave structure.

Our goal is to investigate this effect of beam focusing on the self-excitation of pasotrons both theoretically and experimentally. Our paper is organized as follows. Section II contains formulation of the conditions of self-excitation in pasotrons. In Sec. III an electron motion of a pinching electron beam in the absence of RF oscillations is discussed. (This motion is treated in the previous section as a zero-order approximation for electron coordinates and momenta.) Results of the studies are given in Sec. IV and discussed in Sec. V. Finally, Sec. VI contains the summary. Derivation of the conditions of self-excitation of em oscillations in pasotrons is given in the Appendix.

II. CONDITIONS OF SELF-EXCITATION

In the Introduction, we used Eq. (2) for describing the temporal evolution of the em field amplitude. To simplify our introductory discussion, that equation was given in a simple but general form without discussing all features of the non-stationary process of self-excitation in detail. Below we will treat this formalism in a more accurate manner. Since the derivation of self-excitation conditions for microwave oscillators from Maxwell equations is a standard procedure, we do not reproduce it here. In the Appendix, however, we describe the transformation of the source term (gain function) responsible for em field excitation for the case of pasotrons and also discuss corresponding linearized equations for electron 3D motion. In this section, we only present this self-consistent set of equations describing the pasotron self-excitation in its final form.

This self-consistent set of equations consists of the balance equation, which determines the start current, and linearized equations for electron motion, describing perturbations in electron motion under the action of em oscillations of a small amplitude. To carry out this linearization, let us represent the electron momentum, \vec{p} , which is normalized to mc , the energy normalized to the rest energy, γ , and the phase with respect to the phase of the synchronous harmonic of the backward wave, $\theta = \omega t - k_{z,\text{synchron}}z$, as

$$\vec{p} = \vec{p}_{(0)} + \alpha \vec{p}_{(1)}, \quad \gamma = \gamma_{(0)} + \alpha \gamma_{(1)}, \quad \theta = \theta_{(0)} + \alpha \theta_{(1)}. \quad (13)$$

Here $\alpha = e|A_{\text{synchron}}|/mc\omega$ is the normalized amplitude of the synchronous harmonic acting upon electrons (we assume $\alpha \ll 1$) and subscripts (0) and (1) describe the unperturbed electron motion and perturbations caused by the em field in this motion, respectively. Since in pasotrons both the unperturbed and perturbed motions are 3-dimensional, we should consider not only axial but also radial motion of electrons.

The unperturbed electron phase in pasotrons is axially dependent

$$\frac{d\theta_{(0)}}{dz'} = \frac{1}{\beta_{z(0)}(z')} - h \quad (14)$$

(here $z' = \omega z/c$ is the normalized axial coordinate, $\beta_{z(0)}$ is the unperturbed electron velocity $v_{z(0)}$ normalized to the speed of light c and $h = k_{z,\text{synchron}}c/\omega$ is the normalized axial wave number) first, because the axial component of the electron velocity in a radially diverging/converging beam varies along z -axis and, second, because the potential energy of such a beam, whose space charge field is not completely compensated by ions, is also variable. Therefore, Eq. (14) can be rewritten as

$$\frac{d\theta_{(0)}}{dz'} = \Delta_0 - \frac{1}{\beta_{z0}} \frac{\delta\beta_z}{\beta_{z0}}, \quad (15)$$

where $\Delta_0 = 1/\beta_{z0} - h$ is the detuning of synchronism between the wave and electrons having an initial velocity $\beta_{z0} = v_{z0}/c$ at the entrance and $\delta\beta_z$ describes variation in the electron axial velocity because of the reasons discussed above. This deviation can be determined by the following equation:

$$\frac{\delta\beta_z}{\beta_{z0}} = -\frac{eU(r)}{mc^2\gamma_0^3\beta_{z0}^2} - \frac{1}{2} \frac{\beta_{r(0)}^2}{\beta_{z0}^2}, \quad (16)$$

where $U(r)$ is the potential due to not fully compensated beam space charge and $\beta_{r(0)}$ is the normalized radial electron velocity in the zero-order approximation, which will be discussed later.

Let us consider a resonator formed by a rippled-wall cylindrical waveguide with strong end reflections. As shown in the Appendix, perturbations in components of electron momentum, electron energy and phase caused by the em field of such a resonator can be determined by the following equations:

$$\begin{aligned} \frac{dp_{z(1)}}{dz'} &= \frac{1}{\beta_{z(0)}} \text{Re}\{e^{i\theta}(\kappa I_0 - i\beta_{r(0)}I_1)\}, \\ \frac{dp_{r(1)}}{dz'} &= -\text{Re}\left\{e^{i\theta}I_1\left(\frac{h}{\beta_{z(0)}} - 1\right)\right\}, \\ \frac{d\gamma_{(1)}}{dz'} &= \text{Re}\left\{e^{i\theta}\left(\kappa I_0 - i\beta_{r(0)}\frac{h}{\beta_{z(0)}}I_1\right)\right\}, \\ \frac{d\theta_{(1)}}{dz'} &= -\frac{1}{\gamma_0\beta_{z(0)}^2}(p_{z(1)} - \beta_{z(0)}\gamma_{(1)}). \end{aligned} \quad (17)$$

Here $\kappa = |k_{\perp,\text{synchron}}|c/\omega$ is the normalized absolute value of the transverse wave number of the synchronous em field and I_0 and I_1 are modified zero-order and first-order Bessel functions of the argument κr , respectively.

The balance equation, which determines the start current, can be written in accordance with Eq. (3) [see also Eq. (A18)] as

$$\hat{I}_b \Phi' = 1. \quad (18)$$

In Eq. (18) Φ' is the real part of the gain function determined in the framework of the linear theory [see Eq. (A19)] as

$$\Phi = \frac{i}{S_b} \int_{S_{\perp}} \varphi(r) ds_{\perp} \left\{ \frac{1}{2\pi} \int_0^{2\pi} \left[\int_0^{z_{out}} e^{-i\theta_{(0)}} \theta_{(1)} dz \right] d\theta_0 \right\}. \quad (19)$$

Here the function $\varphi(r)$ describes the radial profile of the beam current density at the entrance. Also, \hat{I}_b in Eq. (18) is the normalized beam current parameter equal to

$$\hat{I}_b = \frac{eI_b}{mc^3} \frac{c^3|a_1|^2}{\omega^3 N_s} \frac{\kappa^2 \langle I_0^2 \rangle}{p_{z0}^3} 2Q_s. \quad (20)$$

Here the coefficient a_1 determines the amplitude of the synchronous first space harmonic and angular brackets designate averaging of the beam coupling coefficient over the interaction cross section (see the Appendix for detail). The product $\hat{I}_b \Phi'$ whose value, in accordance with Eq. (18), determines the start current we will call the excitation factor and denote by Γ .

Coming back to Eqs. (18) and (19) it is necessary to emphasize that, although these equations have a form standard for the equations describing the self-excitation of em oscillations in various microwave sources, their meaning for pasotrons is quite specific. Indeed, in the case of pasotrons, the beam dynamics depends on the time dependent ion focusing, which, in turn, depends on the beam current. Therefore, parameters that were constant for conventional microwave sources are time and beam current dependent in the pasotron theory, i.e., they depend not only on the current rise time, but also on the nominal current value.

So, in this section we have formulated equations describing the pasotron self-excitation conditions. However, so far we did not describe the motion of electrons in an ion-focused beam in the absence of em fields (zero-order approximation) in detail. This will be done in the next section.

III. ELECTRON MOTION IN AN ION-FOCUSED, PHASE-MIXED BEAM

Electron motion in an ion-focused beam in the absence of em fields has been studied in [6,12], where the self-consistent theory of these processes was developed with the account for ion motion. Therefore, referring interested readers to those references, we will outline below the most important results of this theory.

The potential created by a not fully compensated beam space charge, which appeared above in Eq. (16), can be determined as

$$U(r,t) = 2I_{b,nom} \frac{p(t) - f(t)}{v_0} \int_r^{R_w} \frac{I(r')}{I_{b,nom} r'} dr'. \quad (21)$$

Here the function $p(t) = I_b(t)/I_{b,nom}$ describes the beam current pulse shape and the function $f(t) = ev_0 N_i / I_{b,nom} \ll p(t)$ determines the charge compensation ratio; here the ion density per unit length is related to the electron beam density per unit length for the nominal beam current.

The radial coordinate of electrons is determined by the known equation [6,9], which can be given as

$$\frac{d^2 r}{dz^2} = \frac{2I_b}{I_A} \frac{1}{\gamma^2 \beta_{z0}^2} [p(\tau) - \gamma^2 f(\tau)] \frac{1}{r} \frac{I(r)}{I_b} + \frac{\varepsilon^2}{r^3}, \quad (22)$$

where $I_A = (mc^3/e)\gamma\beta_{z0}$ is Alfvén current and ε is the beam emittance determined elsewhere [9].

As shown in [7], the space charge compensation ratio $f(\tau)$ obeys the following equation:

$$\frac{df}{d\tau} = p - 2\Lambda \sqrt{p-f} e^{-(p-f)/\phi}. \quad (23)$$

Here $\phi = T_i v_0 / e I_{b,nom}$ is the normalized ion temperature that, in turn, obeys the equation

$$\frac{d\phi}{d\tau} = \frac{p}{f} \left[\frac{1}{4}(p-f) - \phi \right] - \Lambda \sqrt{p-f} (p-f-\phi) e^{-(p-f)/\phi}. \quad (24)$$

In Eqs. (23) and (24) the time variable t is normalized to the ionization time $t_{ion} = \langle n_g \rangle \sigma v_0$, which is determined by the ion-

ization cross section of a given neutral gas σ and its mean density averaged over the entire interaction volume $\langle n_g \rangle = \int_0^L n_g(z) dz / L$. Of course, such characterization of the ionization time is valid only for the cases when the ionization time is much larger than the time of the ion transit through the interaction region. Also, these equations contain the parameter

$$\Lambda = \frac{1}{2\pi a \langle n_g \rangle \sigma v_0} \sqrt{\frac{2e I_{b,nom}}{M v_0}}, \quad (25)$$

which is the ratio of the characteristic charge compensation time to the half period of ion transverse oscillations. In accordance with the assumption about slow ionization made above, this parameter should be large, $\Lambda \gg 1$. [In Eq. (25) M is the ion mass.]

So, Eqs. (21)–(25) form the set of equations that should be used for characterizing the unperturbed electron motion given above by Eqs. (15) and (16).

IV. RESULTS

The series of calculations has been carried out for typical pasotron parameters. It was assumed that a beam leaving the plasma gun region has a flat radial profile, and two cases of initial beam radius, a_0 , had been considered: 4 cm, which was the radius in the first set of experiments, and 2.25 cm, which was the radius in an optimized pasotron configuration that yielded about 50% efficient operation [4]. The parameter Λ given by Eq. (25) was taken equal to 30, and it was checked in several simulations that at $\Lambda > 10$ the exact value of Λ has very little effect on the results. The beam voltage was 40 kV and calculations had been done for various values of the beam current in the range from 38 to 115 A. We assumed that the operating frequency is 1.3 GHz, the cavity entrance is located at 30 cm away from the electron gun, and the cavity length is equal to 40 cm. Also, the beam emittance in Eq. (22), which can be expressed via the spread in electron transverse velocities or in the orbital-to-axial velocity ratios, $\alpha_0 = v_{\perp 0} / v_{z0}$, as $\varepsilon = a_0 \sqrt{\langle \alpha_0^2 \rangle}$ (see, e.g., [9]), corresponded to 4°–5° angular velocity spread. All these numbers correspond to typical experimental parameters of pasotrons [3,4,7]. In our simulations we used modified Eqs. (15), (17), and (19). These modifications took into account the temporal evolution of electron motion in the zero-order approximation.

As an example of obtained results, the normalized excitation factor $\Gamma = \hat{I}_b \Phi'$ is shown in Fig. 1 as the function of the initial detuning of synchronism Δ_0 for several instants of time normalized to the ionization time t_{ion} . As one can see, while the peak values of this excitation factor at different instants of time are quite different, optimal values of the detuning of synchronism are almost the same.

Temporal evolution of this factor is shown for the optimal detuning of synchronism $\Delta_0 = -3.0$ in Fig. 2 for parameters used in Fig. 1. Here solid line shows the excitation factor for the realistic case, i.e., when the radial nonuniformity of the em field and radial motion of electrons are taken into account; dashed line shows the same function for the case when the radial component of the em electric field and the

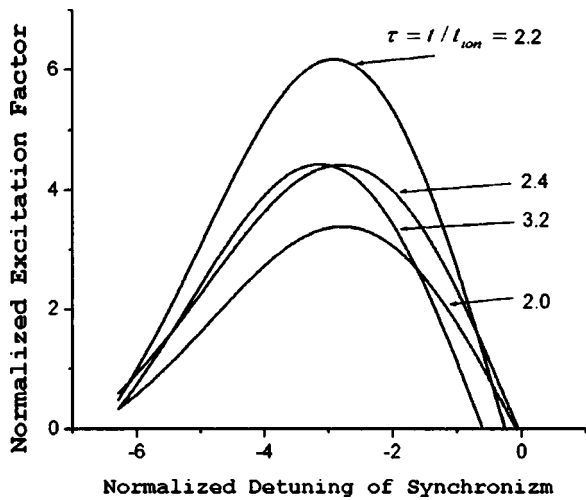


FIG. 1. Excitation factor as the function of the normalized detuning of the Cherenkov synchronism Δ_0 for several instants of time during the beam current rise. The time shown in the figure is normalized to the ionization time. Calculations were done for $I_{b,nom} = 100$ A, $a_0 = 4$ cm and the structure radius 4 cm.

radial nonuniformity of the axial component of this field are neglected. Finally, dotted line here shows the assumed time evolution of the beam current, i.e., the function $p(\tau)$. As follows from Fig. 2, for the parameters chosen, the radial motion of electrons and the radial nonuniformity of the em field play an important role. Our studies also showed that at smaller initial beam radius and radius of a slow-wave structure the effect of the radial nonuniformity is not so strong.

Our formalism has been developed for the case when the current rise time is on the order of the ionization time or larger. Therefore, the self-excitation condition depends on both, the absolute value of the beam current and the current rise time. The excitation factor Γ , which determines this condition, is shown in Fig. 3 as the function of the beam current

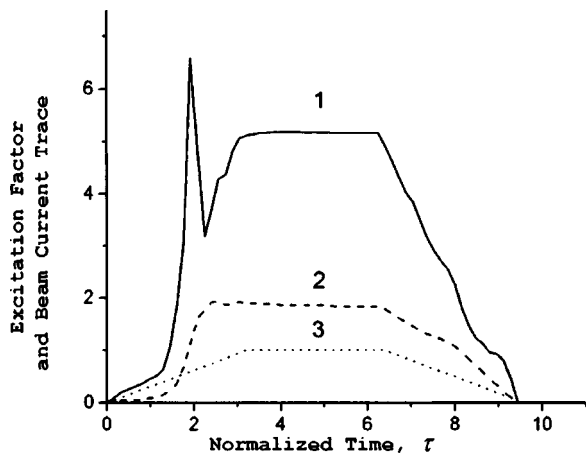


FIG. 2. Time evolution of the normalized excitation factor in the cases when the radial component of the em electric field and the radial nonuniformity of the axial component of this field are taken into account (solid curve 1) and when they are ignored (dashed curve 2). Curve 3 shown by dotted lines depicts the shape of the beam current including the rise and fall times.

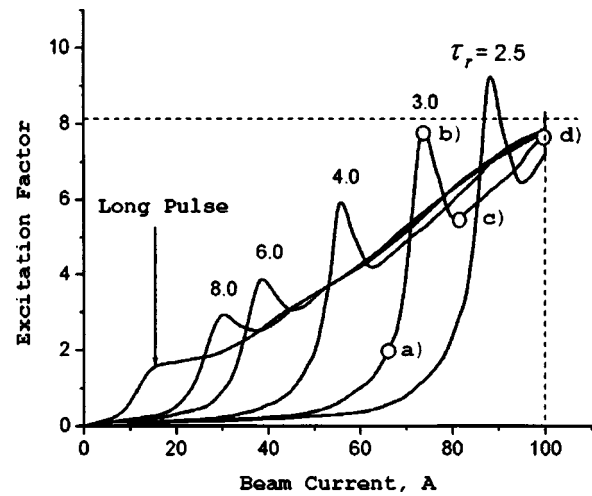


FIG. 3. Evolution of the normalized excitation factor with the increasing beam current in a pasotron with a 100 A nominal beam current (shown by a thin vertical dashed line) for different ratios of the beam current rise time to the ionization time.

for several values of the rise time normalized to the ionization time. While in conventional microwave oscillators the excitation factor $\Gamma = \hat{I}_b \Phi'$ is a linear function of the beam current, since the function Φ (19) is constant in the case of stationary motion of electrons in strong focusing magnetic fields, in pasotrons the product $\hat{I}_b \Phi'$ is not a linear function of the beam current. It is close to this linear function when the beam current rise time is much larger than the ionization time (see the curve labeled "long pulse" in Fig. 3). However, at short rise times, this dependence is not monotonic and is sharper than in the case of a slow current rise. As was discussed in Introduction, this sharpness shortens the rise time of em oscillations. Moreover, it may happen that just the temporal increase of the excitation factor due to the evolution of the radial profile of a pinching beam will cause the pasotron excitation that would be impossible in the case of stationary electron motion. This statement is illustrated in Fig. 3 by a dashed horizontal line, which corresponds to a threshold of oscillations. As shown in Fig. 3, when the current rise time is short enough (see curve for $\tau_r = 2.5$), the self-excitation conditions can be fulfilled in such a pasotrons at currents in a small range between 85 and 90 A, while the device cannot be excited in the case of pulses with longer rise times.

The reason for the appearance of the peak in the curves shown in Fig. 3 for short rise times is obvious from the snapshots shown in Fig. 4. Here the beam focusing and injection into the interaction space shown by dashed lines are shown for several instants of time. At a certain instant of time [Fig. 4(b)], almost all electrons are injected into the interaction space and propagate close to the wall, i.e., just in the region where the beam coupling to the slow wave is maximal. This explains the nonmonotonic behavior of some curves shown in Fig. 3. The formation of the beam focus and the axial motion of the focal plane towards the gun are illustrated by Figs. 4(c) and 4(d). Note that the beam injection in the near-axis region shown in Fig. 4(d) can result in the efficiency enhancement [13].

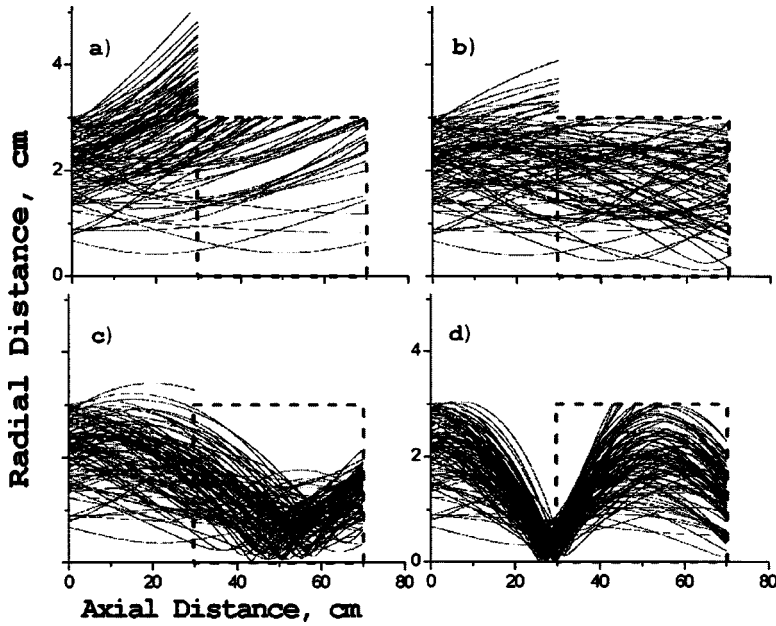


FIG. 4. Several snapshots illustrating the evolution of the beam current transport during the current rise. Corresponding points (a)–(d) are shown in Fig. 3.

Our formalism has allowed us to analyze the relation between the beam current and the start current for different rise times, which was observed experimentally. These experiments were carried out under the same conditions as those described in Ref. [7] where the electron beam dynamics in pasotrons was studied and Ref. [4] where the generation of 0.5 MW peak power with the efficiency in the range from 40% to 50% was reported. Experimental data are summarized in Table I where the start current is given for several values of the beam current and corresponding values of the rise time. As shown in Table I, the current rise time depends on the nominal value of the beam current. This specific feature of the plasma gun is not in the focus of our study, however, interested readers can be referred to [3] where the operation of this plasma gun and corresponding electrical circuitry are discussed in detail.

Theoretical dependencies of the self-excitation conditions on the beam current, which correspond to these experimental data, are shown in Fig. 5 for several values of the nominal beam current and normalized rise time. The dashed horizontal line shows there the threshold, over which the self-excitation starts. Since to determine the normalizing coefficient in Eq. (20) and the ionization time used in our theory by experimental means is quite difficult, it was assumed that, first, we can match our theoretical results with experimental data for the case of the nominal beam current equal to 38 A when the current rise time is very large (50 μ sec). As shown in Table I, the start current in this case is equal to 31 A. Thus,

TABLE I. Experimental data.

| $I_{b,nom}$ (A) | t_{rise} (μ sec) | I_{st} (A) |
|-----------------|-------------------------|--------------|
| 38 | 50 | 31 |
| 57 | 22 | 36.5 |
| 80 | 12 | 45 |
| 115 | 8.4 | 70 |

in accordance with Eq. (3), we determined the threshold as the value of the excitation factor at 31 A. Then, for other nominal currents, we determined the normalized rise times corresponding to crossing of this threshold line by normalized excitation factor curves. It was found that the relations between these normalized times (0.159:0.25:0.417:1.0 for the peak beam currents 115 A, 80 A, 57 A and 38 A, respectively) are very close to the relations between real rise times (0.168:0.24:0.44:1.0) given in Table I. Moreover, relation between real and normalized rise times allowed estimating the ionization time, $t_{ion} \approx 10 \mu$ sec, for this set of experiments. This estimate coincides with one obtained earlier in Ref. [11] where it was found that in a different pasotron experiment the beam reaches its stationary state in 8–10 μ sec.

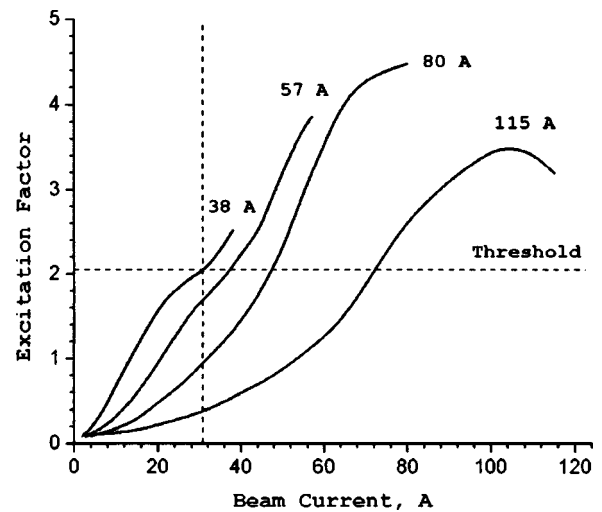


FIG. 5. Evolution of the normalized excitation factor during the current rise time for several values of the nominal beam current. A thin dashed horizontal line shows the threshold for excitation of em oscillations. Intersection of solid lines with this threshold determines the starting current.

V. DISCUSSION

We have found that in pasotrons with the ionization time on the order of the beam current rise time the self-excitation of em oscillations has some specific features, which are uncommon for conventional microwave sources. To describe the self-excitation of em oscillations under such variable conditions, one should use the formalism developed in the present paper and do not rely on the traditional formalism, which was recently applied to pasotrons in Ref. [14]. Our results predict that the onset of em oscillations in pasotrons can take place in a shorter time scale than in conventional microwave sources with similar operating parameters. The fact that during the current rise time the excess of the excitation factor over the threshold can be larger than that for a stationary beam can lead to a possibility to drive an oscillator to the region of hard self-excitation through the region of soft self-excitation. This feature can be important for efficient operation because in a number of cases the maximum efficiency corresponds to the region of hard self-excitation [15] (see also Ref. [1] for the analysis of similar effects in gyrotrons). To verify whether this takes place in the experimental pasotron configuration, it is necessary to develop a large-signal theory of the pasotron operation and carry out corresponding simulations. This will be a topic of our future work.

VI. SUMMARY

It is shown that in pasotron microwave sources with the ionization time on the order of the beam current rise time the self-excitation of em oscillations has some features uncommon for conventional microwave sources, viz., in the process of pasotron excitation not only the beam current increases (as in conventional sources), but also the starting current varies. These specific features of pasotron self-excitation are due to simultaneous temporal variation in the beam current, impact ionization of a neutral gas and corresponding pinching of a beam by created ions. It should be noted that transport of a beam with a moveable focus through the interaction structure can be organized in such a way that, first, a beam with a focus located far from the entrance to the interaction space can propagate close to a slow-wave circuit and, hence, have a strong coupling to the slow-wave. This results in a small start current. Then, in the process of further ionization the focus moves closer to the plasma gun and, correspondingly, a stronger focused beam reduces its coupling to the slow wave. This, in turn, increases the value of the beam current, which is optimal for efficient operation, and, hence, allows one to realize highly efficient operation at high power levels. Agreement between theoretical results and experimental data, which was demonstrated in this paper, indicates that the developed theory adequately describes the most important features of self-excitation of em oscillations in pasotrons.

ACKNOWLEDGMENTS

This work was sponsored by the Air Force Office of Scientific Research (New World Vistas program, Grant No. F496209710270), by the U.S.-Israel Bi-national Science

Foundation, Grant No. 2000140, and by the AFOSR/EOARD, Grant No. FA 8655-03-3006.

APPENDIX: DERIVATION OF THE SELF-EXCITATION CONDITIONS FOR PASOTRONS

Let us consider an excitation of em oscillations in an arbitrary cavity by an arbitrary electron beam and represent the cavity em fields and the electron beam current density, respectively, as

$$\vec{E} = \text{Re}\{A\vec{E}_s(\vec{r})e^{i\omega t}\}, \quad \vec{H} = \text{Re}\{A\vec{H}_s(\vec{r})e^{i\omega t}\}, \quad \vec{j} = \text{Re}\{\vec{j}_\omega e^{i\omega t}\}. \quad (\text{A1})$$

Here A is the complex amplitude of the em field. Equation for this amplitude can be derived from Maxwell equations in a standard way, and it has a form similar to Eq. (2):

$$\frac{dA}{d(\omega t)} = A \left[S - \frac{1}{2Q} - i \frac{\omega - \omega'_s}{\omega} \right]. \quad (\text{A2})$$

In Eq. (A2) ω'_s is the real part of the cold-cavity frequency $\omega_s = \omega'_s + i\omega'_s/2Q$ that slightly differs from the oscillation frequency ω . Also in Eq. (A2) S is the source term proportional to the gain function whose real part Φ' was used in Eq. (2). This term is equal to

$$S = - \frac{1}{2\omega AN_s} \int_V \vec{j}_\omega \vec{E}_s^* dv. \quad (\text{A3})$$

Here $N_s = (1/4\pi) \int_V |\vec{E}_s|^2 dv$ is the norm of the mode of choice. If we use the charge conservation law, $j dt = j_0 dt_0$, where $j_0(r) = j_0 \varphi(r)$, i.e., the function $\varphi(r)$ describes the radial distribution of the beam current density at the entrance to the interaction space [this function is normalized to the beam cross-section area, $\int_S \varphi(r) ds_\perp = S_b$] then Eq. (A3) for this source term can be rewritten as

$$S = - \frac{I_b}{CS_b} \int_S \varphi(r) \left\{ \int_0^{Z_{end}} \left[\frac{1}{\pi} \int_0^{2\pi} \frac{\vec{v} \vec{E}_s^*}{v_z} e^{-i\omega t} d(\omega t_0) \right] dz \right\} ds_\perp. \quad (\text{A4})$$

Here I_b is the absolute value of the beam current, while above the electron current density was negative.

Now we should derive the equations for electron motion. For the sake of simplicity, we will consider a rippled-wall SWS with strong end reflections, in which our e -beam interacts with a symmetric TM_{0p} mode. This mode has only three nonzero field components:

$$E_{sz} = \sum_{n=-\infty}^{\infty} i a_n \frac{g_n}{k} J_0(g_n r) e^{-ik_{zn}z} + \text{c. c.},$$

$$E_{sr} = \sum_{n=-\infty}^{\infty} a_n \frac{k_{zn}}{k} J_1(g_n r) e^{-ik_{zn}z} + \text{c. c.},$$

$$H_{s\varphi} = \sum_{n=-\infty}^{\infty} a_n J_1(g_n r) e^{-ik_{zn}z} + c. c. \quad (\text{A5})$$

Here a_n is the amplitude of the corresponding space harmonic (assume that $a_0=1$). As shown in [16], for our SWS with shallow ripples this amplitude is proportional to the height of ripples l :

$$a_1 = -i \frac{l J_1(g_0 R_0) (g_0^2 + h_0 2\pi/d)}{2 |g| I_0(|g| R_0)}, \quad (\text{A6})$$

also $k_{zn} = k_{z0} + n2\pi/d$ is the axial wave number of this harmonic (d is the period of our SWS), and the transverse wave number is determined by $g_n^2 = k^2 - k_{zn}^2$. (Corresponding field components and amplitudes of space harmonics in a helix slow-wave structure can be found elsewhere [13].) For electron motion the only important is the synchronous first space harmonic of this field. Corresponding field components are equal to

$$\begin{aligned} E_{sz,n=1} &= -a_1 \kappa I_0(\kappa r') e^{-ihz'} + c. c., \\ E_{sr,n=1} &= ia_1 h I_1(\kappa r') e^{-ihz'} + c. c., \\ H_{s\varphi,n=1} &= ia_1 I_1(\kappa r') e^{-ihz'} + c. c. \end{aligned} \quad (\text{A7})$$

Here κ and h are the absolute value of the transverse wave number and the axial wave number normalized to $k = \omega/c$, respectively, primes denote normalization of coordinates to $k = \omega/c$.

Representing the perturbations caused by this field in electron motion as

$$\vec{p} = \vec{p}_{(0)} + \alpha \vec{p}_{(1)}, \quad \gamma = \gamma_{(0)} + \alpha \gamma_{(1)},$$

where $\alpha = e|a_1 A|/mc\omega$ is the normalized amplitude of the first space harmonic acting upon electrons, one can represent the equations for perturbations in the normalized axial and radial components of the electron momentum and the electron energy as

$$\begin{aligned} \frac{dp_{z(1)}}{dz} &= \frac{1}{\beta_{z(0)}} \text{Re} \left\{ e^{i\theta} (\kappa I_0 - i\beta_{r(0)} I_1) \right\} \\ \frac{dp_{r(1)}}{dz} &= -\text{Re} \left\{ e^{i\theta} i I_1 \left(\frac{h}{\beta_{z(0)}} - 1 \right) \right\}, \\ \frac{d\gamma_{(1)}}{dz} &= \text{Re} \left\{ e^{i\theta} \left(\kappa I_0 - i\beta_{r(0)} \frac{h}{\beta_{z(0)}} I_1 \right) \right\}. \end{aligned} \quad (\text{A8})$$

Here momentum components are normalized to mc , γ is the electron energy normalized to mc^2 , primes for coordinates are omitted and subscript (0) denotes an unperturbed 2D motion of electrons. The phase $\theta = \omega t - k_{z,n=1}z$ is determined by the equation

$$\frac{d\theta}{dz'} = \frac{1}{\beta_z} - h. \quad (\text{A9})$$

Here, so far, we did not distinguish the unperturbed motion and perturbations in the electron axial velocity. Once we do this and express perturbations in the electron velocity via the perturbations in the electron axial momentum and electron energy, we can write separately the equation for the unperturbed phase

$$\frac{d\theta_{(0)}}{dz'} = \frac{1}{\beta_{z(0)}} - h \quad (\text{A10})$$

and for the perturbations

$$\frac{d\theta_{(1)}}{dz'} = -\frac{1}{\gamma_0 \beta_{z(0)}^2} (p_{z(1)} - \beta_{z(0)} \gamma_{(1)}). \quad (\text{A11})$$

The boundary condition for the unperturbed phase at the entrance is $\theta_{(0)}(0) = \theta_0$. It is also convenient to shift this phase by ψ , which is determined by $a_1 A = |a_1 A| e^{i\psi}$, i.e., to use $\theta_{(0)} = \theta_{(0)} + \psi$. As a matter of fact, this was already used in Eq. (A8).

Now we can come back to Eq. (A4) and rewrite it in new notations. Taking into account the fact that we consider the paraxial electron motion, let us neglect the transverse interaction. This reduces the integral in square brackets of Eq. (A4) to

$$\frac{1}{\pi} \int_0^{2\pi} E_{s,n=1}^* e^{-i\omega t} d(\omega t_0) = -a_1^* \kappa \frac{1}{\pi} \int_0^{2\pi} I_0(\kappa r') e^{-i\theta} d\theta_0. \quad (\text{A12})$$

Here, in principle, we still may have perturbations caused not only by perturbations in the phase, but also perturbations in the electron radial motion. However, taking into account our assumption about paraxial motion and also our assumption about small radial non-uniformity of the em field, we will neglect the latter. Then, Eq. (A12) can be rewritten as

$$ia_1^* \alpha \kappa I_0(\kappa r) \frac{1}{\pi} \int_0^{2\pi} e^{-i\theta_{(0)}} \theta_{(1)} d\theta_0. \quad (\text{A13})$$

Here we took into account that the zero-order term equals zero after averaging.

Now we can come back to the original equation for the field excitation and, introducing the normalized beam current parameter

$$\hat{I}_b = \frac{e I_b c^3 |a_1|^2}{mc^3 \omega^3 N_s} 2Q_s, \quad (\text{A14})$$

rewrite it as

$$i \frac{\omega - \omega'_s}{\omega/2Q_s} + 1 = \hat{I}_b \Phi, \quad (\text{A15})$$

where the source term is now represented via the gain function given by

$$\Phi = \frac{i}{S_b} \int_{S_\perp} \varphi(r) ds_\perp \left\{ \frac{1}{2\pi} \int_0^{2\pi} \left[\int_0^{Z_{out}} e^{-i\theta_{(0)}} \kappa I_0 \theta_{(1)} dz \right] d\theta_0 \right\}. \quad (A16)$$

One can easily check that in the case of a 1D motion this source term results in the standard monotron function of the transit angle $\Theta = \Delta_0 L$ where $\Delta_0 = 1/\beta_{z0} - h$. The unperturbed phase $\theta_{(0)}$ here is determined by Eq. (A10), and the perturbation in phase is determined by Eq. (A11), in which the perturbations in the axial momentum and energy are given by Eq. (A8).

When the radial nonuniformity of the em field is negligibly small, we can absorb κI_0 present in Eqs. (A8) and (A16) in a new normalized beam current parameter, which will again reduce the number of parameters characterizing the device performance. This means the use of

$$\frac{dp_{z(1)}}{dz} = \frac{1}{\beta_{z(0)}} \text{Re}\{e^{i\theta_{(0)}}\}, \quad \frac{d\gamma_{(1)}}{dz} = \text{Re}\{e^{i\theta_{(0)}}\} \quad (A17)$$

instead of Eq. (A8),

$$\bar{I}_b = \frac{e I_b c^3 |a_1|^2 \kappa^2 \langle I_0^2 \rangle}{m c^3 \omega^3 N_s p_{z0}^3} 2 Q_s \quad (A18)$$

instead of Eq. (A14) (here $p_{z0} = \gamma_0 \beta_{z0}$ and $\langle I_0^2 \rangle$ corresponds to a certain mean value of the zero-order modified Bessel function squared in the interaction space) and

$$\Phi = \frac{i}{S_b} \int_{S_\perp} \varphi(r) ds_\perp \left\{ \frac{1}{2\pi} \int_0^{2\pi} \left[\int_0^{Z_{out}} e^{-i\theta_{(0)}} \theta_{(1)} dz \right] d\theta_0 \right\} \quad (A19)$$

instead of Eq. (A16).

So, all what is left here from our 2D motion and pinching process is (a) the variable axial velocity in Eq. (A10) defining the unperturbed electron phase, (b) the radial profile of the beam current density at the entrance given in Eq. (A19) by the function $\varphi(r)$, and (c) the fact that the interaction length for electrons moving not only axially but also radially can be smaller than the resonator length. Possibly, we can also eliminate γ_0 and $\beta_{z(0)}$ from some equations; however, the perturbation in phase determined by Eq. (A11) contains the difference between two perturbations; thus, here the variation in the unperturbed electron phase along the z axis can be important.

[1] G. S. Nusinovich *et al.*, IEEE-PS **32**, 841 (2004).
 [2] B. Levush and T. M. Antonsen, Jr., IEEE-PS **18**, 260 (1990).
 [3] D. M. Goebel *et al.*, IEEE-PS **22**, 547 (1994).
 [4] A. G. Shkvarunets *et al.*, Phys. Plasmas **9**, 4114 (2002).
 [5] W. H. Bennett, Phys. Rev. **45**, 890 (1934).
 [6] Yu. P. Bliokh and G. S. Nusinovich, IEEE-PS **29**, 951 (2001).
 [7] Y. Carmel, A. Shkvarunets, G. S. Nusinovich, J. Rodgers, Yu. P. Bliokh, and D. M. Goebel, Phys. Plasmas **10**, 4865 (2003).
 [8] J. D. Lawson, *The Physics of Charged-Particle Beams* (Oxford University Press, Oxford, U.K., 1977).
 [9] M. Reiser, *Theory and Design of Charged Particle Beams* (Wiley, New York, 1994), pp. 278–281.
 [10] G. I. Budker, *CERN Symposium on High Energy Accelerators, Geneva, Switzerland* (CERN, Geneva, 1956), Vol. I, p. 68.
 [11] E. S. Ponti, D. M. Goebel, and R. L. Poeschel, *Intense Microwave Pulses IV, Proc. SPIE* Vol. 2843 (SPIE, Bellingham, WA, 1996), p. 240.
 [12] Yu. P. Bliokh, G. S. Nusinovich, J. Felsteiner, and V. L. Granatstein, Phys. Rev. E **66**, 056503 (2002).
 [13] T. Abu-elfadl *et al.*, IEEE-PS **30**, 1126 (2002).
 [14] D. I. Trubetskov and A. E. Khramov, Plasma Phys. Rep. **30**, 80 (2004).
 [15] G. S. Nusinovich and Yu. P. Bliokh, Phys. Plasmas **7**, 1294 (2000).
 [16] N. F. Kovalev, Elektron. Tekh., Ser. 1, Elektron. SVCh. **3**, 102 (1978).